Individual behavior and pairwise interactions between microswimmers in anisotropic liquid

Andrey Sokolov, Shuang Zhou, Oleg D. Lavrentovich, and Igor S. Aranson

Phys. Rev. E **91**, 013009 — Published 15 January 2015

DOI: 10.1103/PhysRevE.91.013009

Individual behavior and pairwise interactions between microswimmers in anisotropic liquid

Andrey Sokolov,[1] Shuang Zhou,[2] Oleg D. Lavrentovich,[2] and Igor S. Aranson[1,*]

[1]*Materials Science Division, Argonne National Laboratory, Illinois 60439, USA*

[2]*Liquid Crystal Institute and Chemical Physics Interdisciplinary Program, Kent State University, Kent, OH 44242, USA*

A motile bacterium swims by generating flow in its surrounding liquid. Anisotropy of the suspending liquid significantly modifies the swimming dynamics and corresponding flow signatures of an individual bacterium and impacts collective behavior. We study the interactions between swimming bacteria in an anisotropic environment exemplified by lyotropic chromonic liquid crystal. Our analysis reveals a significant localization of the bacteria-induced flow along a line coaxial with the bacterial body, which is due to strong viscosity anisotropy of the liquid crystal. Despite the fact that the average viscosity of the liquid crystal is two to three orders of magnitude higher than the viscosity of pure water, the speed of bacteria in the liquid crystal is of the same order of magnitude as in water. We show that bacteria can transport a cargo (a fluorescent particle) along a predetermined trajectory defined by the direction of molecular orientation of the liquid crystal. We demonstrate that while the hydrodynamic interaction between flagella of two close-by bacteria is negligible, the observed convergence of the swimming speeds as well as flagella waves phase velocities may occur due to viscoelastic interaction between the bacterial bodies.

PACS numbers: 47.63.Gd, 05.65.+b, 47.57.Lj, 87.17.Jj

Introduction

Swarms of swimming bacteria exhibit a wealth of remarkable phenomena, from the emergence of large-scale collective behavior to dynamic reduction of viscosity [1, 2] and actuation of microscopic objects [3, 4]. Collective swimming in concentrated bacterial suspensions is being actively investigated, both experimentally and theoretically [5–9]. While the hydrodynamics of swimming microorganism in isotropic fluid is fairly well understood [10–12], the behavior of motile microorganisms in anisotropic environments represented by lyotropic chromonic liquid crystal (LC) was considered only recently [13–16]. Anisotropic visco-elastic properties of LCs significantly modify the individual (cell-liquid) and collective interactions between the swimmers. As it was shown in [14, 16], elongated bacteria align with and swim along the local nematic director orientation. This can be explained by minimization of elastic energy of the liquid crystal around an elongated body and by anisotropy of effective viscosity that is typically lower for motion parallel to the director than perpendicular to it [16–18]. In comparison to an isotropic environment, collective behavior in LC emerges at a significantly lower concentration of bacteria due to long-range orientational ordering [16].

The LC anisotropy is expected to impact the motility of microorganisms at several levels: a) it can modify the flow field around an individual bacterium, b) it can alter pairwise interactions between microswimmers through viscoelasticity of the surrounding medium, and c) it can eventually affect the collective behavior on a larger scale. In this work, we focus on the first two parts of the problem and study experimentally (i) the flow structure created by swimming bacteria; (ii) speed of bacteria in liquid crystalline and isotropic environment; (iii) relationship between the bacterial speed and the frequency of flagellum rotation; (iv) synchronization of swimming speed of two neighboring bacteria.

Our study reveals that an individual bacterium triggers nematic flows that are strongly localized along the axis parallel to the bacterial body. This localization, together with the fact that the bacterium swims along the direction of molecular orientation (the so-called director) leads to an interesting effect of potential significance for applications. Namely, individual bacteria show an ability to push small cargo particles in front of them along a predetermined trajectory defined by the nematic director. The flow localization and cargo transportation are not observed for bacteria swimming in an isotropic fluid such as water, their natural habitat. Swimming velocities measured for bacteria in liquid crystalline medium are only about 2 times smaller than in water despite the fact that the viscosities of the two media differ dramatically. A similarity between swimming in the liquid crystal and pure water is that in both cases the bacterium's velocity is a linear function of the flagellum rotation frequency. Finally, two neighboring bacteria show convergence of swimming velocities and phase velocities of the flagella waves. We attribute this non-trivial effect to LC mediated elastic interactions.

Experiment

Bacteria *Bacillus subtilis* (strain 1085) were inoculated on a LB agar plate and stored at temperature 4 C. Prior to the experiment, bacteria were extracted from an isolated colony and transferred to a 15 ml plastic tube filled

*Electronic address: aronson@anl.gov

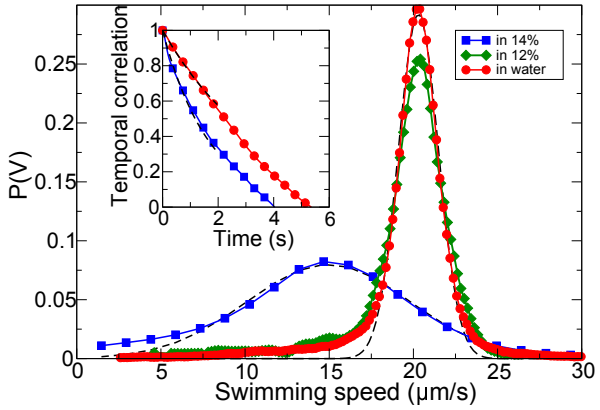

FIG. 1: (Color online) Probability distributions of bacteria swimming speeds in water (red circles), in 12% solution of DSCG in water (isotropic phase, green diamonds) and in 14% solution of DSCG in water (nematic phase, blue squares). Dashed lines are Gaussian fits. Inset: Time autocorrelations of swimming speed in water (red circles) and LC (blue squares). Dashed lines show exponential fits.

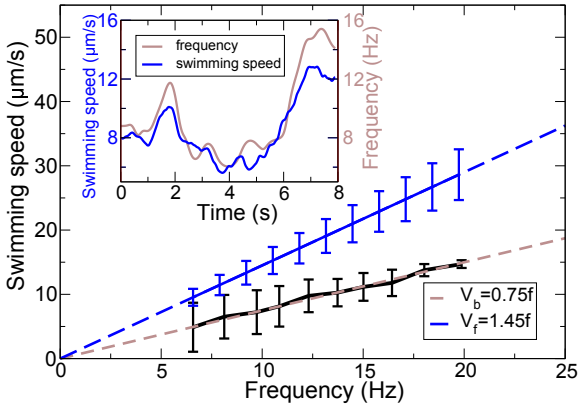

FIG. 2: (Color online) Relationship between the swimming speed and flagella frequency. Black line represents the dependence of a bacterium swimming speed on flagella frequency in LC. Dashed brown (light gray) line shows linear fit. Phase speed of flagella wave as a function of flagella frequency is shown by blue (dark gray) line. Inset: Example of time fluctuations of swimming speed and flagella frequency for an individual bacterium.

with Terrific Broth growth medium and placed in a shaking incubator. For an optimal growth rate, bacteria were incubated at 35C. Concentration of bacteria during incubation period was monitored by measurement of suspension's optical opacity with infra-red proximity sensor. At the end of their exponential stage, the bacteria were extracted from the growth medium by centrifugation and then washed.

The experiments were performed in a planar glass cell of 5-10 μm thickness. Two rectangular glass plates (10×15 mm) were treated with polyamide SE7511 and then gently rubbed with a velvet cloth to ensure uniform alignment of the LC director. Photocurable, biocompatible glue mixed with spherical particles of fixed diameter was used to assemble a glass cell of the required thickness. Chromonic lyotropic LC material disodium cromoglycate (DSCG, Spectrum Chemicals) of 98% purity was dissolved in Terrific Broth to achieve the weight ratio of $14 - 16\%$. At that concentration the obtained mixture is in a nematic phase at room temperature [19]. Bacteria were transferred in this solution and mixed with LC in a vortex mixer at $1,500 - 3,000$ rpm. The resulting solution was sucked into a glass cell by a vacuum pump connected to an opened side of the glass cell. A small air bubble (4-7 mm in diameter) provided oxygen for respiration of *B. subtilis*. The cell was sealed with a vacuum grease to prevent evaporation of water from LC. Since concentration of bacteria in our experiments was very low, no noticeable gradient of oxygen concentration due to respiration of bacteria was created. *B. subtilis* remain motile in LC for 8-12 hours. The duration of a typical experiment was less than 10 minutes. No noticeable change in the behavior of bacteria was detected in the course of experiment. The bacterial dynamics in LC was acquired by an inverted microscope Olympus IX71 with a motorized stage and Prosilica GX 1660 camera ($1{,}600 \times 1{,}200$ pixels) with a frame rate up to 100 fps (using binning 2×2). Displacements of the bacteria, fluorescent markers and flagella dynamics were tracked by a custom MATLAB script.

Results

Distributions of swimming speeds

We first performed a series of experiments to elucidate the speed of bacterium and the rotation frequency of the flagella in three different media: (I1) water (Terrific Broth) ; (I2) water(Terrific Broth) with added 12 wt% of DSCG; (N) nematic phase, representing water with added 14 wt % of DSCG. The first two media are isotropic, the third is a nematic. Note that the difference between the concentration of DSCG in (I2) and (N) is relatively small, only 2 wt%. Comparison of the media (I2) and (N) allows us to analyze and eliminate the possible role of the "chemical shock" associated with the addition of DSCG to water. Remarkably, in both isotropic media, the bacteria show tumbling behavior, while in the LC, they move along the average direction of molecular orientation (the director). Absence of tumbling in the liquid crystal is associated with the fact that the

bacterium must realign itself perpendicular to the director, which causes an elastic energy barrier on the order of $KL \approx 5 \times 10^{-17}$ J, where $K \approx 10$ pN is the elastic constant of the chromonic liquid crystal [20], and $L \approx 5\mu$m is the bacterium length. This barrier is much higher than the typical torque 10^{-18} J of the flagella motor that powers tumbling in an isotropic fluid where the medium imposes no elastic resistance to bacterium's reorientation. In order to accurately represent the bacteria swimming speed, each bacterium was tracked at least 10 sec in the field of view. Firstly, we measured time autocorrelation function of bacterial swimming speed in LC (14% wt of DSCG) and in water and extracted the corresponding characteristic fluctuation times, see Fig 1 (inset). One sees that due to a much higher motor load in LC, the correlation time of a flagella motor $\tau_{LC} = 1.7s$ is roughly half the correlation time in water $\tau_w = 3.61s$. To characterize the magnitude of swimming speed fluctuations we calculated the time probability distribution function for the swimming speed of N different bacteria. Since average swimming speed of individual bacterium varies, in order to obtain an average over the ensemble distribution, each individual function was rescaled to obtain the same average swimming speed V_a (i.e. to satisfy $\int_0^\infty P_n(V) V \, \mathrm{d}V = V_a$). We have chosen $N = 26$ bacterial trajectories in LC and $N = 90$ trajectories in isotropic medium (I1, Terrific Broth) for the purpose of our analysis.

Comparison of different media shows that the speed of bacteria is practically the same in both isotropic media (Terrific Broth and the isotropic phase of DSCG water solution). The only difference between the isotropic media is a somewhat slightly wider distribution of speeds in the DSCG solution, Fig 1. In the (N) medium, the average swimming speed of bacteria in LC is $V_{LC} = 14\mu$m/s, being smaller by a factor of 1.5 than the speed in both isotropic fluids, $V_w = 21\mu$m/s. The width of the distribution (standard deviation) in LC $\sigma_{LC} = 4.8\mu$m/s is four times larger than $\sigma_w = 1.2\mu$m/s in water, Fig 1.

The chromonic liquid crystal is characterized by an anisotropic viscosity. One can identify three different viscosity coefficients, corresponding to the director deformations of splay, bend, and twist. At 14% concentration of DSCG, the experimentally determined values are $\eta_{twist} \approx \eta_{splay} \approx 6$ kg m^{-1}s^{-1}, $\eta_{bend} \approx 0.01$ kg m^{-1}s^{-1} [20]. The splay and twist viscosities that should accompany the bacterial motion in the liquid crystal, are roughly three orders of magnitude higher than the viscosity of water, $\eta_{water} \approx 0.001$ kg/(m s)). For (I2)-medium, the isotropic velocity is about $\eta_{I2} \approx 0.003$ kg/(m s)), as estimated from the diffusion coefficients [18]. It has been established experimentally that flagellated bacteria such as *B. subtilis* placed in an isotropic environment stop swimming when the viscosity of the medium reaches 0.06 kg m^{-1}s^{-1} [21, 22]. As clearly seen in Fig.1, much higher viscosity of the liquid crystal, (N)-medium, does not prevent the bacteria from swimming. To understand this effect, we discuss briefly the current models of flagella propulsion.

The explanation of the flagella-induced motility in Newtonian fluids is based on the difference in the effective drag coefficients for perpendicular ($\xi_\perp^f$) and parallel ($\xi_\parallel^f$) displacement of flagella [23] and on the fact that the flagellum is tilted by some angle θ with respect to the bacterium's axis. The bacterium velocity is proportional to the ratio $\xi_\perp^f/\xi_\parallel^f$ (whose maximum value is 2 [23]) and to θ. In LC, the effective drag coefficients differ also because of the medium anisotropy. Both spherical [18, 24] and rod-like objects [25] experience different resistivity when diffusing along ($\xi_\parallel^{LC}$) and perpendicular ($\xi_\perp^{LC}$) to the director $\mathbf{n}$, with the ratio $\xi_\perp^{LC}/\xi_\parallel^{LC}$ varying in the broad range, from 1.1 to 2.5 [18, 25]. Therefore, the swimming speed of the bacterium in a LC would be determined by both the flagella shape and anisotropy of the medium, $v_{LC} \propto v \times \frac{\xi_\perp^{LC}}{\xi_\parallel^{LC}} \times \frac{\theta_{LC}}{\theta}$, where v is the velocity of bacterium in water (Terrific Broth), and θ_{LC} is the angle between a flagellum segment and the axis of bacterium, which is expected to be smaller than θ, because of the elastic nature of the liquid crystal. Furthermore, the LC is also a medium with memory, caused by the elastic nature of the director field and its coupling to the velocity field. For the LC phase of DSCG, the displacement caused by director distortions decay over a broad range of timescales below 1 sec [18]. Typical frequency of the flagella rotation in LC is 16 Hz, thus we expect that the director relaxation would influence the swimming velocity. To summarize, there are three distinct features of LC that might influence the bacterial speed, namely, anisotropy of viscosity, elastic straightening of the flagellum, and elasticity-mediated short-time memory. The intrinsic anisotropy of LC viscosity might be responsible for the relatively high speed of propulsion, while the elasticity-mediated memory can be responsible for the broad distribution of swimming speeds.

In our earlier work [16] we have found that rotating 24 nm thick bacterial flagella create a pattern of alternating bright and dark spots in polarized light due to the birefringence of LC. This technique enables direct visualization of rotating bacterial flagella. In contrast, if a bacterium becomes temporally non-motile, flagella-induced disturbances of director are much weaker to be detected by the polariziation microscopy (see Movie 1 in [26]). The period of this structure is defined by the pitch of a flagella bundle and according to our measurements is about $d = 2.2 \pm 0.2$ μm, which agrees with fluorescent measurements [27, 28]. Here we monitored the rate of flagella rotation by measuring a frequency of light intensity alternation at a fixed distance from a bacterium tail (see [16] for details). 14 bacterium tracks, where the flagella wave can be reliably detected, were processed. As a result, we observe that the frequency of rotation varies in the course of swimming in LC, Fig 2 (inset). The bacteria swimming speed V_b depends almost linearly on the flagella rotation frequency f, $V_b \approx 0.75f$, Fig 2. Shorter

bacteria swim slightly faster than the longer ones due to more optimal force/drag ratio. The phase velocity of flagella wave in a stationary frame of reference is roughly $V_f = df - V_b = 1.45f \approx 1.93V_b$. Bacteria swimming speed in LC is only two times slower than the phase speed of flagella. For comparison, the average swimming speed of *B. subtilis* in water is about $V_b = 20\mu$m/s, the flagella rotation rate is above 100Hz. Therefore, the phase velocity of flagella wave, $V_f = 200\mu$m/s, is 10 times higher than the swimming speed V_b. Such a difference suggests that fluid flow created by a bacterium swimming in LC is localized along a line coaxial with the bacterial body, a mechanism that makes the propulsion more efficient.

Bacteria-tracer interaction

To further understand the flow field around an swimming bacterium, we use fluorescent markers(polystyrene spheres of diameter 0.25μm doped with fluorescent dye "Nile Red", Spherotech) dispersed in a mixture of liquid crystal and bacteria as indicators. We observed the motion of bacteria and fluorescent signal from tracers by a combination of bright field and fluorescent microscopy. Our measurements reveal that the bacteria interact hydrodynamically with the tracers at distances much larger than the bacterial length when the tracers lay on the bacteria trajectories. The tracers start to move when their separation distance is about $x = 50 - 80\mu$m from the advancing bacterium. Their speed is continuously increasing until collision with the approaching bacteria, Fig 3 and Movie 2 in [26]. Typically, bacteria move faster after loosing the tracer particle. If the tracer is located off the bacterial trajectory by distance of 1μm or more, it is not propelled by the bacterium. This apparent absence of hydrodynamic entrainment away from the bacterial path in LC confirms a strong concentration of flow streamlines along a narrow channel coaxial with the bacterial body. Thus, bacteria can transport a cargo (a fluorescent particle) along a predetermined trajectory defined by the director of liquid crystal, Fig. 3.

To characterize the bacteria-tracer interaction, we measure the tracer velocity as a function of the bacterium-tracer separation distance x measured along the director. The interaction becomes noticeable at $x \approx 50 - 80\mu$m (i.e about $x \approx 10 - 16L_b$, L_b is the bacterial body length) with an onset of tracer motion, Fig 4. This implies a very slow decay of the bacterial flow over distance along the line coaxial with a body. At $x \approx 10 - 20\mu$m $\approx 2 - 4L_b$, a bacterium and a tracer move with comparable velocities. In an isotropic fluid the flow would decrease by an order of magnitude at similar x/L_{bac} values [11].

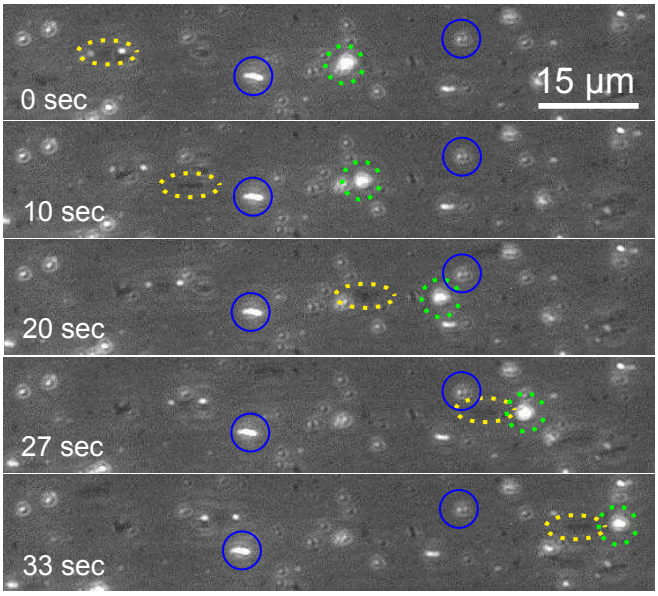

FIG. 3: (Color online) A bacterium (marked by a yellow dashed ellipse) pushes a fluorescent tracer (green dashed circle) located on a bacterial path. Particles located slightly off the bacterial path (marked by solid blue circles) are not advected.

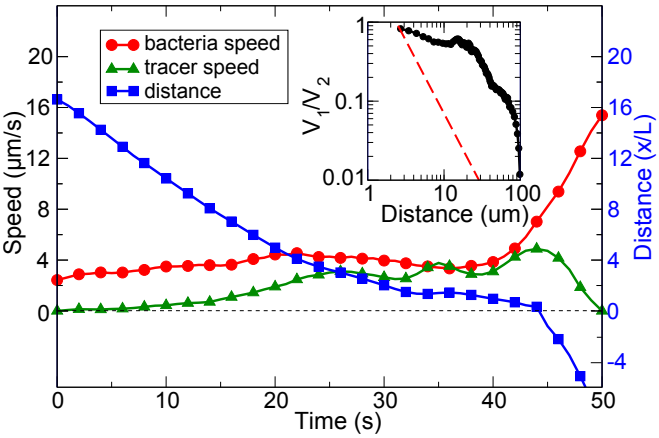

FIG. 4: (Color online) Velocities of a bacterium (red circles) and a tracer (green triangles) and bacterium-tracer distance (blue squares) as a function of time. Bacteria length $L = 5\mu$m. Inset: Decay of the flow magnitude in the direction of swimming normalized by bacteria swimming speed, compared with a typical decay of flow in isotropic liquid (dashed line). Distance is measured from the center of a bacterium.

Flow velocity field

To obtain further insight into the structure of bacteria-generated flow in LC, we reconstruct the flow velocity field from the distorted director pattern around a localized bacterium (see [26] for details). The bacterium is near its division stage, and thus has flagella at both

ends, generating thrusts in opposite directions. As a result, the bacterium drifts around a fixed position along the director direction. The two-dimensional mapping of the director field is obtained by PolScope measurement on a 5μm thick cell with planar alignment. Since the thickness is much smaller than the lateral size of interest (about 100μm), we solve the flow velocity as a 2-D problem using the well established theory of nematodynamics [29], by balancing the elastic torque with the viscous torque. The flow pattern exhibits quadrupolar symmetry, Fig. 5A. The flow along the bacterial body is much stronger than in the perpendicular direction and decays rather slowly, on the scale of micrometers, as can be estimated on the basis of the Leslie-Ericksen nematodynamics, see [26]. Swimming bacterium also exhibits a qualitatively similar "butterfly"-like distortion of the director (compare to flow pattern in [12]), although of a smaller magnitude. This difference can be explained by the fact that an immobilized bacterium "accumulates" over time the stress applied to the same area, while a swimming bacterium does not.

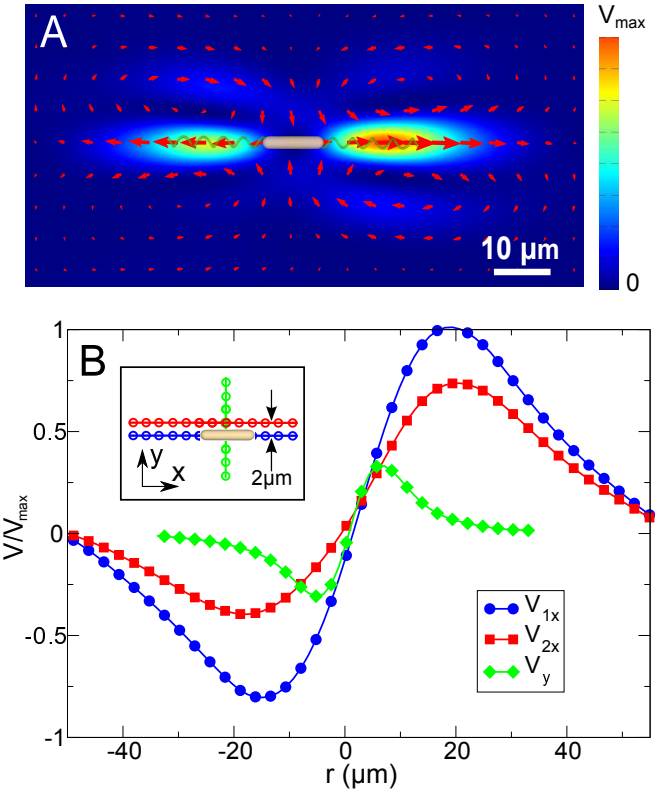

FIG. 5: (Color online) Reconstruction of the flow velocity field. (A) A magnitude of the flow field created by an isolated bacterium in LC. Arrows indicate the direction of flow. (B) Flow profiles, $r = 0$ corresponds to the center of the bacterium. Blue lines (circles) corresponds to horizontal component (parallel to bacterial body) of flow field along the line coaxial with bacterial body (see inset). Red line (squares) corresponds to horizontal component along the line shifted by 2μm in perpendicular direction. Green line (diamonds) represents vertical component of flow along the line perpendicular to bacterial body.

Flagella synchronization

One of the long-standing questions in bacterial coherent swimming is a possibility of frequency and phase locking between the flagella bundles, see e.g. [30, 31]. Synchronous flagella rotation by multiple bacteria may result in a more efficient energy ejection from swimmers into suspension. LC offers a unique opportunity to impose a regime of coherent swimming, as the very fact of bacteria alignment and propulsion parallel to the director suggests long-range interactions. We were able to find multiple protracted events of close encounters between the bacteria that feature some degree of synchronization of their motion (see Movie 3 in [26]). Using a custom MATLAB script we tracked two bacteria swimming next to each other for more than 3 seconds and extracted phase speeds of flagella at each moment of time. For approaching bacteria the difference between their swimming and flagella phase speeds is decreasing, see Fig 6. However, the interaction forces between bacteria are relatively weak and not sufficient to lock the frequencies of flagella and swimming speed for long periods of time. Since our measurements revealed strong localization of hydrodynamic flows on the bacterial body axis (see Figs. 5), the observed convergence of the bacterial speeds and flagella phase velocities is likely due to the elastic interaction mediated by LC. The elastic interactions between bacteria, in turn, originate in director distortions around them and depend on the bacterium shape, surface properties (anchoring) and the state of flagella. When in motion, flagella produce a bundle in a shape of a left-twisted helicoid, counter-clockwise rotation of which propels the cell forward. This shape produces director distortions of a dipolar type [32, 33]. Our estimates (see [26]) for two parallel left-twisted helicoids show that the bacteria might be attracted or repelled from each other by the elastic forces that are by far larger than the thermal energies (4×10^{-21}J) and can be easily comparable (or even larger than) to typical torque of a flagella motor (10^{-18} J) [34].

Conclusion

We have studied flow structure and interactions between bacteria swimming in LC. The study revealed strong flow localization along the bacterial swimming trajectory and possibility of the cargo transport by bacteria, in stark contrast to isotropic liquids [12]. This quasi-one-dimensional signature of the flow affects the interactions between the bacteria on many levels. In particular, it makes the encounters between nearby swimmers more protracted and leads to a noticeable convergence of the bacterial swimming speeds and even flagella phase veloc-

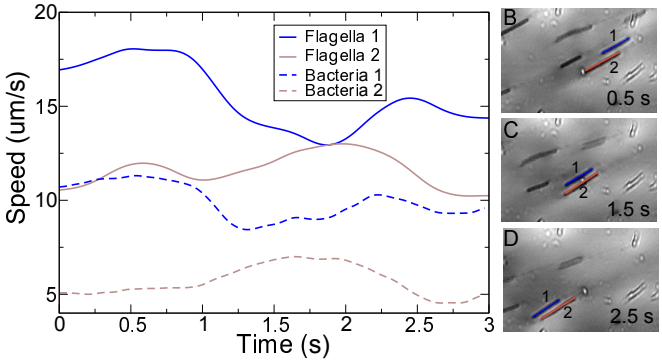

FIG. 6: (Color online) Interaction of nearby bacteria. (A) Swimming speeds (dashed lines) and flagella phase velocities (solid lines) vs time for two bacteria swimming next to each other. Convergence of the flagella phase speeds occurs between 1.5 s and 2 s. (B)-(C) Snapshots of bacteria positions. Bacteria are swimming from right to left. Bacteria marked by numbers corresponding plot (A). See Movie 3 in [26].

ities. However, our measurements do not indicate anticipated phase-locking of rotation frequencies of bacterial flagella motors. The observed phenomenon can possibly be explained by the load redistribution on flagella motors in the course of the encounter (a more slowly moving bacterium is pushed by a faster one, which, in turn, decreases load on the motor and results in increase of its rotation frequency). Detailed mechanism of interaction of swimming bacteria in anisotropic medium is non-trivial and requires further investigation.

Andrey Sokolov and Igor S. Aranson were supported by the US Department of Energy (DOE), Office of Science, Basic Energy Sciences (BES), Materials Science and Engineering Division. Shuang Zhou and Oleg D. Lavrentovich were supported by the National Science Foundation Grants DMR 1104850 (Polscope analysis) and DMS-1434185 (reconstruction of flow patterns and estimates of elastic interactions).

[1] A. Sokolov and I. S. Aranson, Phys. Rev. Lett. **103**, 148101 (2009).
[2] S. D. Ryan, B. M. Haines, L. Berlyand, F. Ziebert, and I. S. Aranson, Phys. Rev. E **83**, 050904 (2011).
[3] L. Angelani, R. Di Leonardo, and G. Ruocco, Phys. Rev. Lett. **102**, 048104 (2009).
[4] A. Sokolov, M. M. Apodaca, B. A. Grzybowski, and I. S. Aranson, Proc. Natl. Acad. Sci. U.S.A. **107**, 969 (2010).
[5] C. Dombrowski, L. Cisneros, S. Chatkaew, R. E. Goldstein, and J. O. Kessler, Phys. Rev. Lett. **93**, 098103 (2004).
[6] A. Sokolov, I. S. Aranson, J. O. Kessler, and R. E. Goldstein, Phys. Rev. Lett. **98**, 158102 (2007).
[7] D. Saintillan and M. J. Shelley, Phys. Rev. Lett. **99**, 058102 (2007).
[8] L. H. Cisneros, J. O. Kessler, S. Ganguly, and R. E. Goldstein, Phys. Rev. E **83**, 061907 (2011).
[9] A. Sokolov and I. S. Aranson, Phys. Rev. Lett. **109**, 248109 (2012).
[10] J. P. Hernandez-Ortiz, C. G. Stoltz, and M. D. Graham, Phys. Rev. Lett. **95**, 204501 (2005).
[11] K. Drescher, R. E. Goldstein, N. Michel, M. Polin, and I. Tuval, Phys. Rev. Lett. **105**, 168101 (2010).
[12] K. Drescher, J. Dunkel, L. H. Cisneros, S. Ganguly, and R. E. Goldstein, Proc. Natl. Acad. Sci. U.S.A. **108**, 10940 (2011).
[13] A. Kumar, T. Galstian, S. K. Pattanayek, and S. Rainville, Molecular Crystals and Liquid Crystals **574**, 33 (2013).
[14] P. C. Mushenheim, R. R. Trivedi, H. H. Tuson, D. B. Weibel, and N. L. Abbott, Soft Matter **10**, 88 (2014).
[15] P. C. Mushenheim, R. R. Trivedi, D. B. Weibel, and N. L. Abbott, Biophysical journal **107**, 255 (2014).
[16] S. Zhou, A. Sokolov, O. D. Lavrentovich, and I. S. Aranson, Proc. Natl. Acad. Sci. U.S.A. **111**, 1265 (2014).
[17] P. Poulin, H. Stark, T. Lubensky, and D. Weitz, Science **275**, 1770 (1997).
[18] T. Turiv, I. Lazo, A. Brodin, B. I. Lev, V. Reiffenrath, V. G. Nazarenko, and O. D. Lavrentovich, Science **342**, 1351 (2013).
[19] J. Lydon, Current opinion in colloid & interface science **3**, 458 (1998).
[20] S. Zhou, K. Neupane, Y. A. Nastishin, A. R. Baldwin, S. V. Shiyanovskii, O. D. Lavrentovich, and S. Sprunt, Soft matter **10**, 6571 (2014).
[21] W. R. Schneider and R. Doetsch, J. Bacteriol. **117**, 696 (1974).
[22] E. Greenberg and E. Canale-Parola, J. Bacteriol. **132**, 356 (1977).
[23] E. Lauga and T. R. Powers, Reports on Progress in Physics **72**, 096601 (2009).
[24] J. Loudet, P. Hanusse, and P. Poulin, Science **306**, 1525 (2004).
[25] B. Senyuk, D. Glugla, and I. I. Smalyukh, Physical Review E **88**, 062507 (2013).
[26] See Supplemental Material at [URL] for additional information and experimental movies.
[27] A. Pijper and G. Abraham, J. Gen. Microbiol. **10**, 452 (1954).
[28] L. H. Cisneros, J. O. Kessler, R. Ortiz, R. Cortez, and M. A. Bees, Phys. Rev. Lett. **101**, 168102 (2008).
[29] P. G. de Gennes and J. Prost, *The Physics of Liquid Crystals* (Clarendon Press, Oxford, 1993), 2nd ed.
[30] M. Kim and T. R. Powers, Phys. Rev. E **69**, 061910 (2004).
[31] G. J. Elfring and E. Lauga, Phys. Rev. Lett. **103**, 088101 (2009).
[32] V. M. Pergamenshchik and V. A. Uzunova, Phys. Rev. E **83**, 021701 (2011).
[33] V. A. Uzunova and V. M. Pergamenshchik, Phys. Rev. E **84**, 031702 (2011).
[34] M. Meister and H. C. Berg, Biophys. Jour. **52**, 413 (1987).